

RESEARCH ARTICLE

Investigation of DNA binding mechanism, photoinduced cleavage activity, electrochemical properties and biological functions of mixed ligand copper(II) complexes with benzimidazole derivatives: synthesis and spectral characterization

Natarajan Raman and Abraham Selvan

Research Department of Chemistry, VHNSN College, Virudhunagar, India

Abstract

The benzimidazole derivative Schiff bases and their copper(II) (Cu(II)) mixed-polypyridyl complexes (**1–4**) have been synthesized and characterized by the spectral and analytical techniques. DNA binding/cleavage studies indicate a stronger binding capability for the complex **4** which is confirmed by the absorbance, viscometric and gel-electrophoresis studies. The photocleavage of plasmid pBR322 DNA reveals that hydroxyl radical (OH[•]) and singlet oxygen (¹O₂) are likely to be the reactive species. Analysis of the growth activity shows that the antimicrobial effect of these Schiff bases on Gram-negative bacteria is higher than that on Gram-positive. Furthermore, the complexes having nitro group show an increased antimicrobial effect.

Keywords: Copper(II) complex, polypyridyl ligand, DNA interaction, antimicrobial study

Introduction

The studies of Copper(II) (Cu(II)) complexes have been widely explored for the versatility of their coordination geometries, exquisite colors, technical application dependent molecular structures, spectroscopic properties and biochemical significance. Octahedral Cu(II) complexes of ligands containing mixed donor atoms have been studied extensively due to their potential applications as molecular materials¹. Fused imidazole derivatives have occupied a prominent place in medicinal chemistry because of their significant properties as therapeutics in clinical applications. Thus, benzimidazole is being explored in the pharmaceutical industries and the substituted benzimidazole derivatives have also been found in the diverse therapeutic applications. In particular, it has been an important pharmacophore and privileged structure in medicinal chemistry. Several platinum complexes with N-heterocyclic ligands, such

as imidazole, thiazole, benzimidazole, benzoxazole and benzothiazole, have been reported². It has been also suggested that the azomethine linkage is responsible for the biological activities of Schiff bases such as, antitumor, antibacterial, antifungal and herbicidal activities³.

Transition metal complexes that cleave DNA under physiological condition are of current interest in the development of artificial nucleases. Most studies of nucleic acid cleavage by the small molecules have been focused on oxidative cleavage and photocleavage. However, these oxidative cleavage agents require the addition of an external agent (light, oxidative and/or reductive agent) to initiate cleavage. The DNA fragments generated by the hydrolytic cleavage can be enzymatically ligated and endlabeled. Small metal complexes that promote the hydrolytic cleavage of DNA could be useful not only in molecular biology and drug design, but also in elucidating the precise role of metal ions in enzyme

Address for Correspondence: Research Department of Chemistry, VHNSN College, Virudhunagar-626 001, India. Tel.: +091-092451-65958; Fax: +091-4562-281338. E-mail: drn_raman@yahoo.co.in

(Received 02 April 2011; revised 17 May 2011; accepted 17 May 2011)

catalysis. One of the most important DNA-related activity of the transition metal complexes is that, some of the complexes show the ability to cleave DNA. Very recently, Cu(II) complexes have been reported to be active in DNA strand scission⁴.

Studies on the interaction of transition metal complexes with DNA continue to attract the attention of researchers due to their importance in design and development of synthetic restriction enzymes, chemotherapeutic drugs and DNA foot printing agents⁵. Binding of small molecules with DNA has been studied extensively since DNA is the material of inheritance and controls the structure and function of cells. In this respect, copper(II) complexes have attracted a great deal of attention due to their strong DNA-binding and potential anticancer⁶.

The present work stems from our interest to develop the chemistry of copper complexes of benzimidazole derivative based ligands. Thus, the available literature encouraged us to synthesize and characterize the Cu(II) metal complexes [containing 1,10-phenanthroline(phen) and 2,2'-bipyridine(pby)] with newly synthesized Schiff bases derived from N,N-bis(benzimidazolyl)oxalate hydrochloride and 4-substituted anilines. The electron transfer mechanism is investigated by the aid of cyclic voltammetry. This paper mainly focuses on exploring the DNA-binding affinities of the above Cu(II) complexes using electronic absorption, cyclic voltammetry and viscosity measurements. Their ability to induce the cleavage of pBR322 DNA in understanding the recognition of DNA by small ligands or metal complexes is crucial for the development of drugs targeted at DNA. We hope the results will be of high value in further understanding of DNA binding, the efficiency of DNA recognition and cleavage by Cu(II) complexes as well as laying the foundation for the rational design of new photoprobes and photonucleases of DNA.

Experimental protocols

Chemistry

All the chemicals used were of analytical grade. The solvents were used after purification by the standard method described in the literature⁷. Benzimidazole, diethyloxalate, 4-nitroaniline, 4-methoxyaniline, 1,10-phenanthroline, 2,2'-bipyridine and Cu(II) chloride salt were used as supplied for the preparation of complexes. Calf thymus DNA (CT DNA) was obtained from the Sino-American Biotechnology Company. Tris-HCl buffer (5 mM Tris-HCl, 50 mM NaCl, pH-7.2, Tris=Tris(hydroxymethyl)aminomethane) solution was prepared by using deionized double distilled water. The concentration of CT DNA was measured by its known extinction coefficient at 260 nm ($6,600 \text{ M}^{-1} \text{ cm}^{-1}$)⁸. The absorbance at 260 nm (A_{260}) and at 280 nm (A_{280}) for CT DNA was measured to ensure its purity. The ratio A_{260}/A_{280} was found to be 1.84, indicating that CT DNA was satisfactorily free from protein⁹.

The spectroscopic titration was carried out in buffer at room temperature. UV-Vis spectra were recorded on

a Shimadzu Model 1601 UV-Visible Spectrophotometer. Cyclic voltammetric measurements were performed at room temperature on a CHI620C electrochemical analyzer in freshly distilled DMF solution. The X-band EPR spectra of the complexes were recorded on a Jeol RE2x electron spin resonance spectrometer at RT (300 K) and LNT (77 K) using TCNE as the g-marker. FTIR spectra were obtained on a Perkin-Elmer Paragon 1000 FTIR spectrophotometer equipped with KBr discs, using the diffuse reflectance technique ($4000\text{--}400 \text{ cm}^{-1}$). Microanalyses were performed on a Perkin-Elmer 240 elemental analyzer. ¹H NMR spectra were recorded on Bruker (300 MHz) spectrometer. Mass spectrometry experiments were performed on a JEOL-AccuTOF JMS-T100LC mass spectrometer equipped with a custom-made electrospray interface (ESI). X-ray diffraction experiments were carried out on XPERT-PRO diffractometer system. Copper $K\alpha_1$ line, with wavelength of 1.5406 \AA generated with a setting of 30 mA and 40 kV with the electrodes, was used for diffraction. The slit width setting was 91 mm. The diffracting angle (2θ) was scanned from 10.0251 to 79.9251 continuously with a rate of 2° per minute. Scanning Electron Micrography study was performed on SEM; JEOL JSM Model 6360 was used for morphological evaluation. Room temperature magnetic susceptibility measurements were carried out on a modified Gouy-type magnetic balance, Hertz SG8-5HJ. The molar conductivity was measured for (10^{-3} M) DMF solution using a conductometer model 601/602.

Synthesis and spectral characterization

Preparation of N,N-bis(benzimidazolyl)oxalate hydrochloride (L_1)

The synthesis route for the ligand L_1 is shown in Scheme 1. Benzimidazole (1.1814 g, 0.01 mol) was dissolved in EtOH (50 mL) and to this solution was added diethyl oxalate (1.4615 g, 0.01 mol) in a 2:1 molar ratio. The solution was refluxed for *ca.* 1 h, and then conc. HCl (6 mL) was added dropwise with constant stirring. The cream crystalline product formed was filtered off under vacuum, washed thoroughly with hexane and dried in *vacuo*.

Yield 85% M.F: $C_{16}H_{10}N_4O_2$, M.Wt: 290.28, Anal. Calcd. (%) C(66.24 %), H(3.56 %), N(19.31 %); found (%) C(66.19 %), H(3.47 %), N(19.28 %); ¹H NMR (300 MHz, $CDCl_3$) δ , ppm: 6.78–7.56 (ArH), IR(KBr) $\gamma(\text{cm}^{-1})$: 1699 (m)(C=O), 1394 (s) (C=N,bz), 1344(w) (C-N,bz), 1448(s) (Ph-C=C), 1529(s) (Ph-C-C), 2872(w) (Ph-C-H).

Preparation of Schiff base ligands L_2^a and L_2^b

The Schiff bases L_2^a and L_2^b were synthesized by refluxing ethanolic solutions of L_1 (2.9028 g, 0.01 mol) with 4-methoxyaniline (2.463 g, 0.02 mol) or 4-nitroaniline (2.7624 g, 0.02 mol) in 20 mL ethanolic solution in a 1:2 molar ratio with a constant stirring. Then the mixture was refluxed for 3–4 h. A solid mass separated was collected and washed by ethanol. Crystallization was done with ethanol and then dried over $CaCl_2$.

L_2^a : black powder, yield 65%, M.F: $C_{30}H_{24}N_6O_2$, M.Wt: 500.55, Anal. Calcd. (%) C(71.83 %), H(4.87 %), N(16.81

); found (%) C(71.97 %), H(4.81 %), N(16.78 %); ^1H NMR (300 MHz, CDCl_3) δ , ppm: 3.42(s, 3H, O- CH_3), 6.72-7.21(m, Ph); IR(KBr) $\gamma(\text{cm}^{-1})$: 1595 (s) (C=N), 1307(s) (O- CH_3), 1446(m) (Ph-C=C), 1521(s) (Ph-C-C), 2868(w) (Ph-C-H); UV-Vis (DMF) [nm(frequency, cm^{-1}) (transition)]; 393(25,445) (intra ligand charge transfer) (ILCT), 267(37,453) (ILCT), 243(41,152) (ILCT), 229(43,668) (ILCT).

L_2^b : greenishyellow powder, yield 58%, M.F: $\text{C}_{28}\text{H}_{18}\text{N}_8\text{O}_4$, M.Wt: 530.50, Anal. Calcd. (%) C(63.41%), H(3.47%), N(21.17%); found (%) C(63.37%), H(3.40%), N(21.12%); ^1H NMR (300 MHz, CDCl_3) δ , ppm: 6.68-7.34(m, Ph); IR(KBr) $\gamma(\text{cm}^{-1})$: 1599(s) (C=N), 1631(m) (C- NO_2), 1471(w) (Ph-C=C), 1504(m) (Ph-C-C), 2827(m) (Ph-C-H); UV-Vis (DMF) [nm(frequency, cm^{-1}) (transition)]; 410(24,390) (ILCT), 243(41,152) (ILCT), 229(43,668) (ILCT).

Synthesis of Schiff base Cu(II) complexes

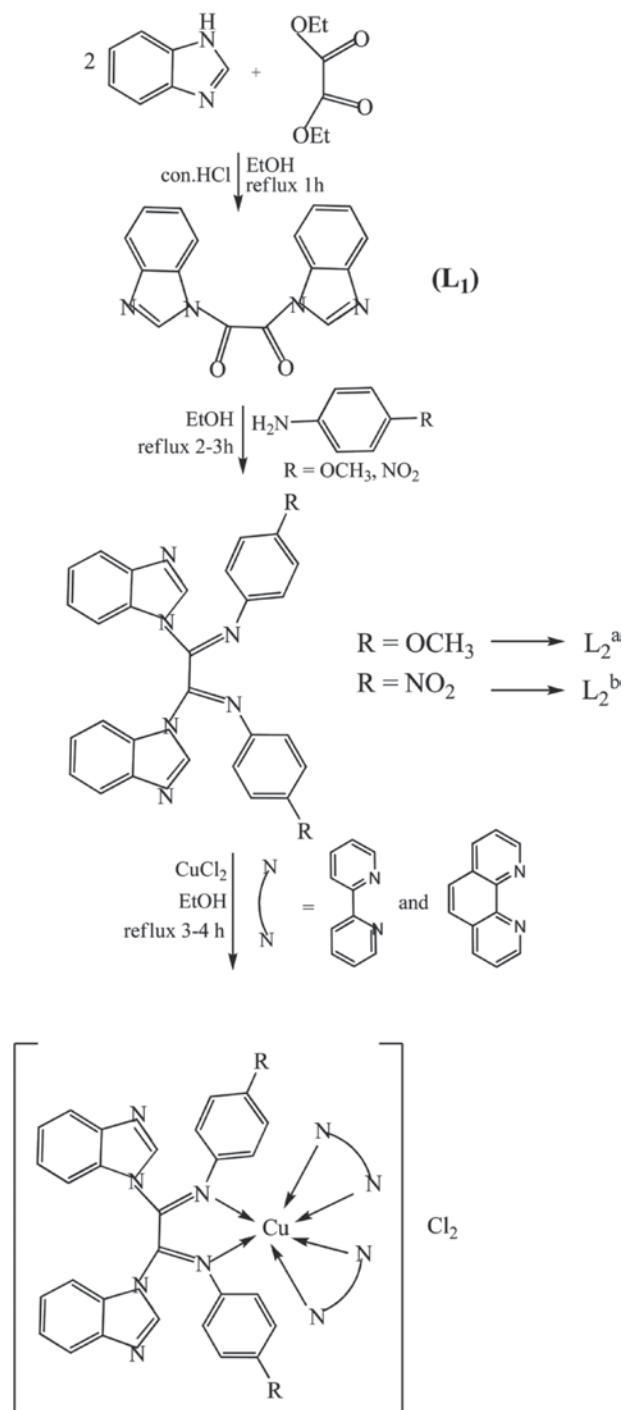
All the new Cu(II) complexes were prepared by the following general procedure described in Scheme 1. To an ethanolic solution of the appropriate Schiff base (0.001 mol), copper chloride salt (0.001 mol) in ethanol (15 mL) was added and kept stirring for 30 min. To the above stirring solution, about 0.002 mol of bpy/phen in the ethanolic solution was added and refluxed for 2-3 h. The resultant solid product was washed and recrystallized with ethanol.

$[\text{CuL}_2^a(\text{bpy})_2]\text{Cl}_2$ (**1**): black powder, yield 78%, M.F: $[\text{CuC}_{50}\text{H}_{40}\text{N}_{10}\text{O}_2]\text{Cl}_2$, M.Wt: 947.38, Anal. Calcd. (%) C(63.43 %), H(4.34 %), N(14.83 %), Cu(6.72 %); found (%) C(63.39 %), H(4.23 %), N(14.79 %), Cu(6.68 %); IR(KBr) $\gamma(\text{cm}^{-1})$: 1546(s) (C=N), 1311(s) (O- CH_3), 1429(w) (Ph-C=C), 1516(s) (Ph-C-C), 2874(s) (Ph-C-H), 406(s) (M-N); UV-Vis (DMF) [nm(frequency, cm^{-1}) (transition)]; 955(10,471) ($^2\text{B}_{1g} \rightarrow ^2\text{B}_{2g}$) Octahedral (O_h), 743(13,459) ($^2\text{B}_{1g} \rightarrow ^2\text{A}_{1g}$) (O_h), 531(18,832) (ILCT), 385 (25,974) (ILCT), 303 (33,003) (ILCT).

$[\text{CuL}_2^a(\text{phen})_2]\text{Cl}_2$ (**2**): black powder, yield 72%, M.F: $[\text{CuC}_{54}\text{H}_{40}\text{N}_{10}\text{O}_2]\text{Cl}_2$, M.Wt: 995.43, Anal. Calcd. (%) C(65.15 %), H(4.07 %), N(14.12 %), Cu(6.38 %); found (%) C(65.12 %), H(4.01 %), N(14.03 %), Cu(6.35 %); IR(KBr) $\gamma(\text{cm}^{-1})$: 1558(m) (C=N), 1303(s) (O- CH_3), 1425(s) (Ph-C=C), 1511(s) (Ph-C-C), 2870(w) (Ph-C-H), 408(s) (M-N); UV-Vis (DMF) [nm(frequency, cm^{-1}) (transition)]; 940(10,638) ($^2\text{B}_{1g} \rightarrow ^2\text{B}_{2g}$) (O_h), 738(13,550) ($^2\text{B}_{1g} \rightarrow ^2\text{A}_{1g}$) (O_h), 522(19,157) (ILCT), 462 (21,645) (ILCT), 291 (34,364) (ILCT).

$[\text{CuL}_2^b(\text{bpy})_2]\text{Cl}_2$ (**3**): green powder, yield 68%, M.F: $[\text{CuC}_{48}\text{H}_{34}\text{N}_{12}\text{O}_4]\text{Cl}_2$, M.Wt: 977.32, Anal. Calcd. (%) C(59.06 %), H(3.56 %), N(17.21 %), Cu(6.54 %); found (%) C(58.96 %), H(3.48 %), N(17.18 %), Cu(6.48 %); IR(KBr) $\gamma(\text{cm}^{-1})$: 1511(w) (C=N), 1620(m) (C- NO_2), 1442(s) (Ph-C=C), 1481(s) (Ph-C-C), 2868(m) (Ph-C-H), 409(s) (M-N); UV-Vis (DMF) [nm(frequency, cm^{-1}) (transition)]; 965(10,363) ($^2\text{B}_{1g} \rightarrow ^2\text{B}_{2g}$) (O_h), 740(13,514) ($^2\text{B}_{1g} \rightarrow ^2\text{A}_{1g}$) (O_h), 387(25,840) (ILCT), 321 (31,153) (ILCT), 281 (35,587) (ILCT).

$[\text{CuL}_2^b(\text{phen})_2]\text{Cl}_2$ (**4**): green powder, yield 75%, M.F: $[\text{CuC}_{52}\text{H}_{34}\text{N}_{12}\text{O}_4]\text{Cl}_2$, M.Wt: 1025.37, Anal. Calcd. (%) C(60.92 %), H(3.41 %), N(16.43 %), Cu(6.21 %); found (%) C(60.89 %), H(3.33 %), N(16.39 %), Cu(6.17 %); IR(KBr) $\gamma(\text{cm}^{-1})$: 1516(s) (C=N), 1629(m) (C- NO_2), 1425(m) (Ph-C=C), 1485(s) (Ph-C-C), 2868(w) (Ph-C-H), 414(s) (M-N); UV-Vis (DMF) [nm(frequency, cm^{-1}) (transition)]; 967(10,341) ($^2\text{B}_{1g} \rightarrow ^2\text{B}_{2g}$) (O_h), 735(13,605) ($^2\text{B}_{1g} \rightarrow ^2\text{A}_{1g}$) (O_h), 385(25,974) (ILCT), 293 (34,130) (ILCT).



Scheme 1. Synthetic route for the preparation of copper complexes.

Biological study

The methods of DNA binding, photoactivated cleavage experiments and pharmacology studies are discussed in supplementary material.

Results and discussion

All complexes were soluble in organic solvents like DMF and DMSO. The synthesized copper complexes were characterized by elemental analyses, IR, UV-Vis, ^1H NMR, mass spectroscopy, magnetic susceptibility measurement, XRD and SEM analysis.

FTIR studies and mode of bonding

The data of the IR spectra of Schiff base ligands L_2^{a} , L_2^{b} and their copper complexes are listed in experimental section. The IR spectra of the complexes are compared with the free ligands in order to determine the coordination sites that may involved in chelation. L_2^{a} and L_2^{b} show a strong band at 1595 and 1599 cm^{-1} respectively due to the imine group vibrations. After complexation, this band is shifted to a lower frequency, in the range 1511–1558 cm^{-1} , supporting the binding of the imine nitrogen with the metal ions¹⁰. Furthermore, no bands for free carbonyls are observed, which indicates that complete condensation has occurred. The presence of sharp band in the region 406–414 in the spectra of all the complexes assigned to $\nu(\text{M-N})$ mode further supports to the involvement of nitrogen atom in coordination¹¹. The IR values, $\nu(\text{C-H})$ 860 cm^{-1} and 735 cm^{-1} observed for phenanthroline are red shifted to 850 cm^{-1} and 721 cm^{-1} . These shifts can be explained by the fact that each of the two nitrogen atoms of phenanthroline ligands donates a pair of electrons to the central metal forming a coordinate covalent bond¹².

Therefore, from the IR spectra, it is concluded that L_2^{a} and L_2^{b} behave as bidentate ligands with NN donor sites and bind to the metal ions through two azomethine N and four nitrogens through two pby/phen as co-ligands.

Magnetic susceptibility and UV-Vis studies

Magnetic susceptibility measurements provide sufficient data to characterize the structure of the metal complexes. The formation of the metal complexes was also confirmed by electronic spectra. The electronic absorption spectra of the Schiff base ligands L_2^{a} , L_2^{b} and their copper complexes were recorded in DMF, over the 200–1100 nm range. The L_2^{a} and L_2^{b} ligands showed strong absorption bands in the ultraviolet region (263–408 nm), that could be attributed respectively to the $\pi \rightarrow \pi^*$ and $n \rightarrow \pi^*$ transitions in the benzene ring or azomethine ($-\text{C}=\text{N}$) groups for free ligand. All the copper complexes showed the intense electronic bands observed in the spectral range 550–1000 nm are assigned to the d-d band, which is in agreement with six-coordinate geometry. The strong band observed in the range 280–550 nm is associated with the imine transition in all the metal complexes¹³. Thus, a comparison of the absorption data of the complexes with

that of the ligands clearly indicates the formation of a metal complex in each case.

The electronic spectra of the **1-4** chelates consist of a band centered at around 967–735 nm, which is consistent with an octahedral configuration. On the basis of electronic spectra, the position of the bands and their weak intensity have assigned them to d-d transitions, $^2\text{B}_{1g} \rightarrow ^2\text{B}_{2g}$ and $^2\text{B}_{1g} \rightarrow ^2\text{A}_{1g}$. This supports the distorted octahedral Cu(II) complex which is usual in the d^9 case¹⁴. These complexes have magnetic moment values in the range 1.96–1.84 BM, which is higher than the spin-only value (1.73 BM) expected for one unpaired electron and offers possibility of an octahedral geometry observed for Cu(II) complexes¹⁵.

Molar conductivity

With a view to study the electrolytic nature of the mononuclear metal complexes, their molar conductivities were measured in DMF (dimethylformamide) for 10^{-3} M solutions at $25 \pm 2^\circ\text{C}$. The molar conductivity values of the copper complexes (**1-4**) are in the range of 52.4–78.3 $\Omega^{-1} \text{cm}^2 \text{mol}^{-1}$ which indicate the ionic nature of these complexes. These high values indicate that mononuclear metal complexes are electrolytes¹⁶ due to presence of counter ions in the proposed structure of the mononuclear metal complexes (Scheme 1).

EPR studies

The EPR spectral assignments of the Cu(II) metal complexes are discussed in supplementary material.

ESI-mass studies

The electron impact mass spectra of L_2^{b} ligand and its complex **3** were recorded and investigated at 70 eV of electron energy. The molecular weights of all the complexes were established from the molecular ion peaks observed in the corresponding ESI mass spectra. The ESI mass spectrum of L_2^{b} Schiff base shows a molecular ion peak m/z at 530 which is equivalent to its molecular weight and also exhibits two additional peaks m/z at 531 and 532 corresponding to $(\text{M} + 1)$ and $(\text{M} + 2)$ peaks, respectively. The ESI mass spectrum of **3** shows a molecular ion (M^+) peak at $m/z = 906$, and also exhibits two additional peaks m/z at 907 and 908, which are corresponding to $(\text{M} + 1)$ and $(\text{M} + 2)$ peaks respectively. The different competitive fragmentation pathways of the complex **3** gave important peaks at m/z 594, 531, 237 ($\text{M} + 2$), 412 and 410 ($\text{M} - 2$) due to the fragments $[\text{CuC}_{28}\text{H}_{18}\text{N}_8\text{O}_4]^+$, $[\text{C}_{28}\text{H}_{18}\text{N}_8\text{O}_4]^+$, $[\text{C}_{14}\text{H}_{11}\text{N}_4]^+$, $[\text{C}_{21}\text{H}_{12}\text{N}_6\text{O}_4]^+$ and $[\text{C}_{21}\text{H}_{10}\text{N}_6\text{O}_4]^+$, respectively. Most of the complexes showed additional peaks corresponding to the fragments formed due to the loss of the metal ion. So, it is reasonable to conclude from the assignment of the fragments of the four studied complexes exist in a monomeric form. The molecular ion peaks shown by these complexes are in good agreement with the structure suggested by elemental analysis, spectral and magnetic studies.

X-ray diffraction and SEM analysis

The structure and surface morphology study of the compounds has been discussed in supplementary file.

Biological study results

Viscosity studies

Viscosity titration measurements were carried out to clarify the interaction modes between the investigated compounds and CT DNA. The classic intercalation model involves the insertion of a planar molecule between DNA base pairs, which results in a decrease in the DNA helical twist and lengthening of the DNA, the molecule will be in close proximity to the DNA base pairs as well. In contrast, groove-face or electrostatic interactions typically cause a bend (or kink) in DNA helix reducing its effective length and thereby its viscosity.

The effects of the Cu(II) complexes **1**, **2**, **3** and **4**, together with ethidium bromide (EB) on the viscosity of rod-like DNA at $25 \pm 2^\circ\text{C}$ are shown in Figure 1. The intercalator ethidium bromide (EB) significantly increases the relative specific viscosity of DNA as expected for the lengthening of the DNA double helix resultant from

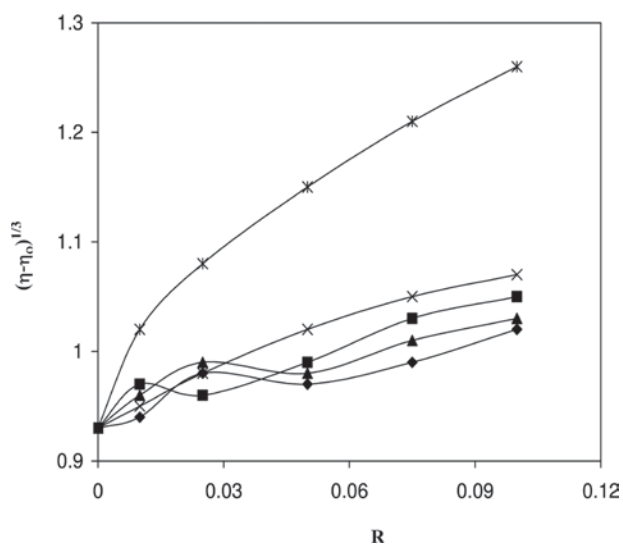


Figure 1. Effect of increasing amounts of EB (*) and in presence of increasing concentration of complexes of **1** (◆), **2** (▲), **3** (■), **4** (×) on the relative viscosity of CT-DNA at $25 \pm 2^\circ\text{C}$. [DNA] = 1.5 mM, $R = [\text{complex}]/[\text{DNA}]$ or $[\text{EB}]/[\text{DNA}]$.

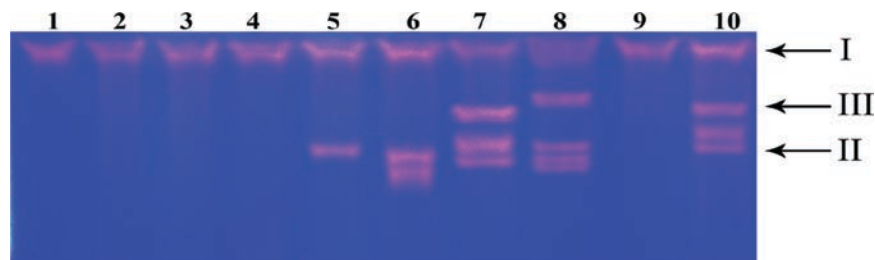


Figure 2. Agarose gel showing cleavage of SC pBR322 DNA (0.2 µg) incubated with 50 µM complexes **1-4** in the presence of 0.25 mM H_2O_2 in Tris-HCl/NaCl buffer (50 mM, pH=7.2) at 37°C for 1.5 h. Lane 1: DNA control; lane 2: DNA + H_2O_2 ; lane 3: DNA + **1**; lane 4: DNA + **4**; lane 5: DNA + H_2O_2 + **1**; lane 6: DNA + H_2O_2 + **2**; lane 7: DNA + H_2O_2 + **3**; lane 8: DNA + H_2O_2 + **4**; lane 9: DNA + H_2O_2 + **4** + DMSO; lane 10: DNA + H_2O_2 + **4** + SOD (4 units).

well-characterized intercalation. This difference of DNA binding model between Cu(II) complexes **1-4** should be caused by the different nature of substituents present in Schiff base ligands of these complexes. For complexes **1** and **2**, due to the bulky methoxy group located in L_2^a ligand may restrict from planarity, these complexes could not completely intercalate into DNA base pairs. The partial intercalation may act as a “wedge” to pry apart one side of a base pair stack, as observed for the $\Delta\text{-[Ru(phen)}_3\text{]}^{2+17}$, but not fully separate the stack as required by the classical intercalation model. This would cause a static bend or kink in the helix and decreases the viscosity of DNA. The complexes **3** and **4**, involve an intercalation mode. This is probably related to the molecular structure of the complex. In complexes **3** and **4**, the bpy/phen ligands and nitro group present in L_2^b ligand moiety, in which complex **4** is somewhat more planarity and completely intercalated with DNA. However, in bpy-Cu(II) complex **3**, the bpy ligands bind DNA weakly through intercalative mode. So, it is likely that the observed slight increase in relative viscosity of these complexes is not due to intercalative interaction but due to partial and/or non classical interaction.

The changed degree of viscosity which follows the order of $\text{EB} > \mathbf{4} > \mathbf{3} > \mathbf{2} > \mathbf{1}$ may depend on its affinity to DNA, which is consistent with electronic absorption spectroscopy studies.

Chemical nuclease activity

The chemical nuclease activities of complexes **1-4** have been studied using supercoiled pBR322 plasmid DNA as a substrate in a medium of 50 mM Tris-HCl/NaCl buffer (pH=7.2) in the presence of hydrogen peroxide as an activator under physiological conditions. All the four complexes **1-4** showed remarkable cleavage. The structure of the ligand plays an important role in the cleavage¹⁸. When circular plasmid DNA is subjected to electrophoresis, relatively fast migration will be observed for the supercoiled form (Form I). If scission occurs on one strand (nicking), the supercoiled form will relax to generate a slowly moving open circular form (Form II). If both strands are cleaved, a linear form (Form III) that migrates between form I and form II will be generated.

The nuclease efficiency of the Cu(II) complexes is known to depend on the activator used for initiating

the DNA cleavage. Several authors have studied the influence of different activators on the cleavage of DNA by Cu(II) complexes¹⁹. In our work, we have found that hydrogen peroxide is the best activator for DNA cleavage. The results of the gel electrophoresis separations of plasmid pBR322 DNA by the complexes **1–4** are depicted in Figure 2. The “chemical nuclease” activity follows the order: **4** (phen)₂ > **3** (bpy)₂ > **2** (phen)₂ > **1** (bpy)₂. Control experiments using the metal complexes alone do not show any apparent cleavage of SC DNA. The bpy complex **1** shows moderate cleavage activity due to its inability to bind to DNA. Complexes **3** and **4** having a DNA intercalator nitro group show good chemical nuclease activity. Control experiments show that the hydroxyl radical scavenger DMSO inhibits the DNA cleavage suggesting the possibility of hydroxyl radical and/or “copper-oxo” intermediate as the reactive species²⁰. SOD addition does not have any apparent effect on the cleavage activity indicating the non-involvement of O₂ in the cleavage reaction. The mechanism involved in the DNA cleavage reactions is believed to be similar to that proposed by Sigman and coworkers for the “chemical nuclease” activity of bis(phen)copper species²¹. The different DNA cleavage efficiency of these four complexes may be due to the different binding affinity of the complexes to DNA.

Photo-induced DNA Cleavage

A number of metal polypyridyl complexes have been shown to exhibit DNA photocleaving ability²². The cleavage of plasmid pBR322 DNA by the Cu(II) complexes can be easily monitored by agarose gel electrophoresis. Complexes **3** and **4** have been found to bring about photocleavage of supercoiled plasmid pBR322 DNA when excited at 365 nm. After the photoexposure, the sample was incubated for 1 h at 37°C, followed by its addition to the loading buffer containing 25% bromophenol blue, 0.25% xylene cyanol and 30% glycerol (3 μL). The solutions were finally loaded on 1.5% agarose gel containing 1.0 μg mL⁻¹ (EB). Electrophoresis was carried out in a dark room for 1.5 h at 80V in Trisacetate-EDTA (TAE) buffer. The bands were visualized by UV light and photographed. Figure S1(A, B) (supplementary material) shows the gel electrophoresis separation of pBR 322 DNA after incubation with complexes (**3** and **4**) and irradiation at 365 nm.

The mechanistic aspects of the DNA cleavage reactions involving complexes **3** and **4** (50 μM) have been investigated at 365 nm wavelength using various control experiments (Figure S1, supplementary material). We investigated the DNA cleavage in the presence of hydroxyl radical scavengers (DMSO, EtOH), singlet oxygen quenchers (NaN₃, L-Histidine), superoxide scavenger (SOD), hydrogen peroxide scavenger (catalase) and chelating agent (EDTA) under our experimental conditions. From Figure S1, it is inferred that no obvious inhibitions are observed for **3** and **4** complexes in the presence of SOD (Lane 7) and catalase (Lane 8), the results rule out the possibility of DNA cleavage by superoxide. The addition of DMSO (Lane 3), EtOH (lane 4), NaN₃ (Lane 5)

and L-Histidine (Lane 6) partly diminishes the nuclease activity of the two compounds which is indicative of the involvement of hydroxyl radical and the singlet oxygen or a singlet oxygen-like entity in the cleavage process. The inhibitory activity of sodium azide can be ascribed to the affinity of the azide anion for transition metals²³. The EDTA, a Cu(II)-specific chelating agent that strongly bind to Cu(II) forming a stable complex, can efficiently inhibit DNA cleavage, indicating Cu(II) complexes play the key role in the cleavage. The Cu(II) complexes examined here may be capable of promoting DNA cleavage through an oxidative DNA damage pathway in the presence of various reagents, in which giving active oxygen species such as hydroxyl radical and singlet oxygen or singlet oxygen-like entity, probably a copper-peroxide that cleaves DNA.

Spectroscopic studies on DNA binding

DNA-binding studies are important for the rational design and construction of new and more efficient drugs targeted to DNA. In these studies, all the compounds were dissolved in 1% DMF and 99% Tris-HCl buffer (5 mM Tris-HCl, 50 mM NaCl, pH 7.2) at a concentration of 25 μM. All the experiments involving the interaction of complexes with CT DNA were carried out in Tris-HCl buffer.

Electronic absorption spectra

The binding of complexes **1–4** to DNA helix has been characterized through absorption spectral titrations, by following changes in absorbance and shift in wavelength. For metallo-intercalators, DNA-binding is associated with hypochromism and a red shift in the ILCT bands. Figure S2, supplementary material) shows Cu(II) complexes in the absence and presence of CT DNA. Addition of increasing amounts of CT DNA results in hypochromism and a red shift. As increasing the concentration of CT DNA, the MLCT transition band of complexes **1** at 530 nm, **2** at 510 nm, **3** at 382 nm and **4** at 381 nm exhibits hypochromism of 6.28%, 6.59%, 19.68% and 24.64%, and bathochromism of 3.5, 4, 4.5 and 5 nm, respectively. These spectral characteristics obviously suggest that complexes **1–4** interact with DNA most likely through an intercalative and/or electrostatic mode that involves a stacking interaction between the aromatic chromophore and the base pairs of DNA.

In order to further elucidate the binding strength of the complexes, the intrinsic constants K_b were determined by monitoring the changes of absorbance in the MLCT band with increasing concentration of CT DNA. The K_b values of copper(II) chelates are 3.22 × 10⁴, 3.71 × 10⁴, 3.77 × 10⁴ and 3.80 × 10⁴ for **1**, **2**, **3** and **4**, respectively, a little difference in DNA-binding affinity of the four Cu(II) complexes can be understood as a result of the fact that the complex with nitro moiety Schiff base ligand shows stronger binding affinity with DNA. This may be due to the high numbers of planar phen ligand and nature of substituent moieties present in the complex²⁴ which

cooperatively act to increase the overall binding ability of the Cu(II) complexes with DNA.

Redox behavior

The redox behavior of the newly synthesized compound $[\text{CuL}_2^{\text{a}}(\text{pby})_2]\text{Cl}_2$, $[\text{CuL}_2^{\text{a}}(\text{phen})_2]\text{Cl}_2$, $[\text{CuL}_2^{\text{b}}(\text{pby})_2]\text{Cl}_2$ and $[\text{CuL}_2^{\text{b}}(\text{phen})_2]\text{Cl}_2$ in TBAP-DMF have been investigated using cyclic voltammetry. Cyclic voltammetry was used to confirm the oxidation levels of the metal centers in the Cu(II) complexes. The electrochemical properties of metal complexes, particularly with nitrogen donor atoms have been studied in order to consider spectral and structural changes accompanying with electron transfer.

The cyclic voltammogram between +0.4 and -0.4 V shows oxidation process Cu(II)/Cu(III) while in the range of 0 to -1.0 V, it shows the reduction process which may be assigned to Cu(II)/Cu(I) couple (Table 1). All of them resemble of a quasi-reversible one-electron transfer process. Cyclic voltammetric technique has been employed to study the interaction of the redox active Cu(II) complexes with DNA in order to further testify the DNA binding modes assessed from the above spectral and viscosity studies. Summaries of voltammetric results of **1-4** complexes are given in Table 1.

In the absence of DNA, the cyclic voltammogram recorded at room temperature shows a quasi-reversible peak for the Cu(II) → Cu(III) couple at 0.439 V and 0.396 V versus Ag/AgCl with a direct cathodic peak for Cu(III) → Cu(II) at -0.145 V and -0.332 V for complexes **1** and **2**, respectively. On titration with DNA, a decrease in peak current with very slight potential shift was observed for complexes **1** and **2**, which is consistent with the non-coordinating intercalative binding of copper complexes through phen/bpy ligand moiety between the DNA base pairs as also evidenced by the spectral results. It is observed from the voltammogram that the ΔE_p values are not much sensitive to the DNA addition, while there is a considerable decrease in peak current as well as in the I_{p_a}/I_{p_c} values. The formal potential, $E_{1/2}$ taken as the average of E_{pc} and E_{pa} shifts slightly towards the negative side on binding to DNA suggest that both Cu(II) and Cu(I) forms bind to DNA at different rates. The drop of the voltammetric currents in the presence of CT DNA can be attributed to diffusion of the metal complex bound to

the large, slowly diffusing DNA molecule. The decrease extents of the peak currents observed for the above two complexes upon addition of CT DNA may indicate that the DNA binding affinity increases in the order: **1** < **2**. The results parallel to the above spectroscopic and viscosity data of these two complexes in the presence of DNA.

In the absence of DNA, the cyclic voltammogram for complex **3** exhibits two quasi-reversible one-electron reduction processes. Inspection of this voltammogram indicates that the first reduction wave at -0.936 V and its corresponding oxidation wave appeared at -0.393 V are related to the Cu(II)/Cu(I) reduction process in the range -0.2 to -1.1 V. Second redox peak potentials for the Cu(III)/Cu(II) couple are found at $E_{pc} = -0.358$ V and $E_{pa} = 0.069$ V. The ratio of anodic to cathodic peak currents I_{p_a}/I_{p_c} was 0.217 and 0.925 V for first and second redox couples respectively. The formal electrode potentials $E_{1/2}$, ΔE_p (difference in cathodic E_{pc} and anodic E_{pa} peak potentials) were -0.664 and 0.543 V for Cu(II)/Cu(I), 0.144 and 0.427 V for Cu(III)/Cu(II) couple, respectively. At constant parameters, the addition of CT-DNA results the shift in $E_{1/2} = -0.639$ V and $\Delta E_p = 0.520$ V for Cu(II)/Cu(I), $E_{1/2} = 0.131$ V and $\Delta E_p = 0.414$ V respectively for Cu(III)/Cu(II) (Fig. S3) (supplementary material). The ratio of I_{p_a}/I_{p_c} is 0.143 and 0.665 for CT-DNA bound metal complex **3**, exhibits first and second redox couples, respectively. The shift in potentials and decrease in current ratio suggest the binding of complex **3** to CT-DNA.

The cyclic voltammetric data of complex **4** in the absence of DNA (Figure S3 B, supplementary material) featured the reduction of Cu(II) → Cu(I) form at a cathodic peak potential. E_{pc} of -0.985 V, and the reoxidation of the Cu(I) form upon scan reversal occurred at -0.116 V and one more reduction peak is appeared at $E_{pc} = -0.425$ V with no corresponding anodic peak. This is possibly because the electron-withdrawing anion makes the complex more positively charged and it favors the reduction of metal ion. Similarly the electron-donating groups make the complexes less positively charged and it favors oxidation to Cu(III). Electropotentials of Cu(III)/Cu(II) couple is showing sensitivity to the nature of atoms in ligands moiety. The higher reduction potential can be attributed due to the greater planarity and electronic properties those are associated with aromatic rings.

Table 1. Redox couples of the complexes, their potentials and the shift of the potentials in the absence and presence of CT-DNA.

Complex	Redox couple	$I_{pc} (\text{A}) \times 10^{-5}$		$E_{pc} (\text{V})$		$E_{1/2} (\text{V})$		$\Delta E_p (\text{V})$		$K_{\text{oxd}}/K_{\text{red}}$
		Free	Bound	Free	Bound	Free	Bound	Free	Bound	
1	Cu(III)/Cu(II)	3.00	2.90	-0.145	-0.132	0.147	0.125	0.584	0.514	1.65
	Cu(II)/Cu(I)	3.24	3.20	-0.796	-0.779	-0.500	-0.503	0.591	0.552	1.94
2	Cu(III)/Cu(II)	0.428	0.409	-0.332	-0.314	0.364	0.329	0.728	0.659	2.01
	Cu(II)/Cu(I)	0.638	0.474	-0.983	-0.953	-0.450	-0.467	0.900	0.934	3.21
3	Cu(III)/Cu(II)	1.04	0.96	-0.358	-0.338	0.144	0.131	0.427	0.414	2.18
	Cu(II)/Cu(I)	2.46	1.51	-0.936	-0.899	-0.664	-0.639	0.543	0.520	4.22
4	Cu(III)/Cu(II)	1.15	0.78	-0.425	-0.404	—	—	—	—	2.26
	Cu(II)/Cu(I)	2.67	1.65	-0.985	-0.935	-0.434	-0.390	0.869	0.780	7.01

Electrochemical data recorded in volt, at room temperature, $E_{1/2} = 1/2(E_{pc} + E_{pa})$.

Upon the addition of Cu(II) complex **4** with DNA, the geometry around the Cu(II) ion in complex is changed due to the interaction of DNA. Therefore, the redox potential of Cu(II)/Cu(I) also changes. CV results show that a new reduction peak appears at higher potential than the original reduction peak which can be attributed to changes in the geometry around copper center in the complex through the binding of Cu(II) compartmental Schiff base complex **4** to DNA. Therefore, our CV results suggest the interaction between DNA and copper complex **4**. According to these observations, it seems that the decrease in peak currents of complex **4** after addition of DNA are caused by the binding of complex **4** to the bulky, slowly diffusing DNA molecule.

The shift in $E_{1/2}$ with increasing amounts of DNA indicates a difference in the binding of Cu(II) and Cu(I) species to DNA. The net shift in $E_{1/2}$ can be used to estimate the ratio of equilibrium constants, K_{2+}/K_{+} for the binding of the Cu(II) and Cu(I) forms, respectively, to DNA. For a Nernstian electron transfer system in which both the oxidized and reduced forms are associated with a third species such as DNA in solution can be applied. Here, Cu^{n+} -DNA represents the copper complex bound to DNA with $n+$ charge on the metal centre. Thus for a one electron transfer,

$$E^{\circ}_b - E^{\circ}_f = 0.0591 \log(K_{2+}/K_{+})$$

where E°_f and E°_b are the formal potentials of the Cu(II)/Cu(I) couple in the free and bound forms, respectively. K_{2+} and K_{+} are the corresponding binding constants for the Cu(II) and Cu(I) species to DNA. For complex **4**, K_{2+} is higher than K_{+} , suggests that the interaction of Cu(II) complexes with DNA tends to stabilize the Cu(II) over the Cu(I) state.

It can be observed that complexes **1-4** exhibit the same electrochemical behaviour upon addition of CT DNA. For increasing amounts of CT DNA, the cathodic potential E_{pc} shows a positive shift ($\Delta E_{pc} = +0.013\text{V}$ for **1**, $\Delta E_{pc} = +0.018\text{V}$ for **2**, $\Delta E_{pc} = +0.020\text{V}$ for **3** and $\Delta E_{pc} = +0.021\text{V}$ for **4**) while the anodic potential E_{pa} shifts to more negative values [$\Delta E_{pa} = -0.057\text{V}$ for **1** (Figure S3A, supplementary material), $\Delta E_{pa} = -0.051\text{V}$ for **2**, $\Delta E_{pa} = -0.007\text{V}$ for **3** for Cu(III)/Cu(II) redox couple], the cathodic potential E_{pc} shows a positive shift ($\Delta E_{pc} = +0.017\text{V}$ for **1**, $\Delta E_{pc} = +0.030\text{V}$ for **2**, $\Delta E_{pc} = +0.037\text{V}$ for **3** and $\Delta E_{pc} = +0.050\text{V}$ for **4**)

while the anodic potential E_{pa} shifts to negative values [$\Delta E_{pa} = -0.022\text{V}$ for **1**, $\Delta E_{pa} = -0.064\text{V}$ for **2**, $\Delta E_{pa} = -0.014\text{V}$ for **3** and $\Delta E_{pa} = -0.039\text{V}$ for **4** (Figure S3 B, supplementary material)] for Cu(II)/Cu(I) redox couple respectively. These shifts of the potentials show that complexes **1-4** can bind to DNA by both intercalation and electrostatic interaction²⁵.

Pharmacology effect

The results of antimicrobial screening of all the newly synthesized compounds are presented in Table 2 (Figure S4, supplementary material). Some of them showed moderate to good activity with MIC values in the range of 5.53–9.26 $\mu\text{g}/\text{mL}$ in DMF. In general, the two Schiff bases have a moderate antimicrobial effect on both antibacterial and antifungal strains, possibly due to the presence of azomethine groups (imines) which have chelating properties. These properties may be used in metal transport across the bacterial membranes or to attach to the bacterial cells at a specific site from which it can interfere with their growth. This is in agreement with Huheey et al.²⁶ who mentioned that antibiotics such as streptomycin, aspergillidic acid, and tetracycline with chelating properties were able to compete successfully with metal-binding agents for bacteria while not disturbing the metal processing by the host and thus interfering with the growth of bacteria.

It was demonstrated that the L_2^b Schiff base showed a higher effect on *E. coli* than *S. aureus* and this difference could be due to the Gram-status. It is known that the membrane of gram-negative bacteria is surrounded by an outer membrane containing lipopolysaccharides. The newly synthesized Schiff bases seem to be able to combine with the lipophilic layer in order to enhance the membrane permeability of the gram-negative bacteria. The lipid membrane surrounding the cell favors the passage of only lipid soluble materials; thus the lipophilicity is an important factor that controls the antimicrobial activity. Also the increase in lipophilicity enhances the penetration of Schiff bases into the lipid membranes and thus restricts further growth of the organism. This could be explained by the charge transfer interaction between the Schiff base molecules and the lipopolysaccharide molecules which lead to the loss of permeability barrier activity of the membrane.

Table 2. Antimicrobial activities of Cu(II) complexes evaluated by MIC (minimum inhibitory concentration, $\mu\text{g mL}^{-1}$).

Complex	Antibacterial activity				Antifungal activity			
	<i>S. aureus</i>	<i>B. subtilis</i>	<i>E. coli</i>	<i>P. aeruginosa</i>	<i>A. niger</i>	<i>R. stolonifer</i>	<i>C. albicans</i>	<i>R. bataticola</i>
L_2^a	21.34	22.06	19.57	23.45	25.03	21.08	24.34	22.12
L_2^b	15.19	17.43	14.28	21.46	17.54	19.42	16.21	19.38
1	7.03	8.11	6.69	8.15	9.26	8.54	7.06	8.41
2	6.11	7.23	6.78	6.41	8.31	7.12	7.63	8.19
3	6.23	7.12	5.53	6.74	8.27	6.47	7.54	8.24
4	5.82	6.94	5.74	6.23	7.75	5.92	6.12	8.16
Streptomycin	3.25	2.87	2.54	3.02	—	—	—	—
Nystatin	—	—	—	—	2.82	3.31	2.45	2.96

The results of anti-bacterial screening reveal that among all the compounds screened, compounds **L**₂^a, **L**₂^b and **1-4** showed moderate anti-bacterial activity while compounds **3** and **4** displayed good anti-bacterial activity when compared with streptomycin used as standard. This finding agrees with Azam et al.²⁷ who mentioned that compounds containing methoxy groups at different positions of the aromatic ring showed less inhibition on microbial growth while compounds having halogens, hydroxyl and nitro groups showed a good inhibitory effect.

In case of antifungal activity, the Schiff bases and their Cu(II) complexes were found to be highly active. All the metal complexes possess higher antifungal activity than the Schiff bases. Complexes **1** and **2** have more antifungal active against *C. albicans* and *R. bataticola*, respectively than **3**, but less active than **4**. This higher antimicrobial activity of the metal complexes compared to Schiff bases may be due to the change in structure due to coordination and chelating tends to make metal complexes to act as more powerful and potent bacteriostatic agents, thus inhibiting the growth of the microorganisms. Moreover, coordination reduces the polarity of the metal ion mainly because of the partial sharing of its positive charge with the donor groups within the chelate ring system formed during the coordination. This process, in turn, increases the lipophilic nature of the central metal atom, which favors its permeation more efficiently through the lipid layer of the microorganism, thus destroying them more aggressively.

Accordingly, the data obtained from this investigation were in good agreement with the previous studies that expressed the metal complexes with Schiff bases have greater activity towards microorganisms. Finally, it suggested that the reason for this higher antimicrobial efficacy can be related to the inhibition of several structural enzymes, which play a key role in vital metabolic pathways of the microorganisms.

Conclusions

In this work, we have synthesized two new bidentate NN donor ligands and their Cu(II) complexes. The Cu(II) ion is coordinated by two azomethine-N atoms and two co-ligand-N atoms to form a six coordinate geometry. Magnetic moment and electronic spectral data indicate a distorted octahedral geometry for the Cu(II) complexes. EPR data reveal that the metal-ligand bonds have considerable covalent character. The DNA binding experiments using electronic spectral technique show the hypochromism and red shift at the charge transfer region. The DNA binding results using cyclic voltammetric experiments suggest that there is good interaction of the complexes with DNA by both intercalation and electrostatic modes. The DNA cleavage studies for the complexes **1-4** reveal that they cleave the DNA through an oxidative (O₂-dependent pathway) cleavage mechanism using the hydroxyl radical and the singlet oxygen as the

reactive species, because DMSO, EtOH, L-Histidine and azide ions are obviously inhibiting the cleavage activity. We have performed a comparative study for the influence of methoxyl and nitro moiety present in the ligands on DNA cleavage activity. Anti-biogram studies witness the prominent activity of copper complexes compared to the activity of ligands.

Acknowledgments

The authors express their sincere thanks to the College Managing Board, Principal and Head of the Department of Chemistry, VHNSN College for providing necessary research facilities. Instrumental facilities provided by Sophisticated Analytical Instrument Facility (SAIF), IIT Bombay and CDRI, Lucknow are gratefully acknowledged.

Declaration of interest

The authors report no conflicts of interest. The authors alone are responsible for the content and writing of this article.

References

- Masoud MS, Amira MF, Ramadan AM, El-Ashry GM. Synthesis and characterization of some pyrimidine, purine, amino acid and mixed ligand complexes. *Spectrochim Acta A Mol Biomol Spectrosc* 2008;69:230-238.
- Nuir MM, Cox O, Rivera LA, Cadiz ME, Medina E. *ChemInform Abstract: synthesis and characterization of new platinum(II) complexes containing thiazole and imidazole donors. Part 3. Dichlorobis(styrylbenzazole) platinum(II) complexes.* *Inorg Chim Acta* 1992;191:131-139.
- Rekha S, Nagasundara KR. Complexes of the Schiff base derived from 4-aminophenyl benzimidazole and 2, 2'-dehydropyrrolidene-N-aldehyde with Zn (II), Cd (II) and Hg (II) halides. *Indian J Chem A* 2006;45:2421-2425.
- Reddy PR, Rao KS, Satyanarayana B. Synthesis and DNA cleavage properties of ternary Cu(II) complexes containing histamine and amino acids. *Tetrahedron Lett* 2006;47:7311-7315.
- Tan LF, Wang F, Chao H, Zhou YF, Weng C. Ruthenium(II) mixed-ligand complex containing 2-(4'-benzyloxy-phenyl)imidazo[4,5-f][1,10]phenanthroline: synthesis, DNA-binding and photocleavage studies. *J Inorg Biochem* 2007;101:700-708.
- Senthil Kumar R, Sasikala K, Arunachalam S. DNA interaction of some polymer-copper(II) complexes containing 2,2'-bipyridyl ligand and their antimicrobial activities. *J Inorg Biochem* 2008;102:234-241.
- Perrin D. D, Armarego W.L.F, Perrin D.R. *Purification of Laboratory Chemicals*, 2nd ed., Pergamon Press, 1981.
- Patra AK, Roy S, Chakravarty AR. Synthesis, crystal structures, DNA binding and cleavage activity of l-glutamine copper(II) complexes of heterocyclic bases. *Inorg Chim Acta* 2009;362:1591-1599.
- Xi PX, Xu ZH, Liu XH, Cheng FJ, Zeng ZZ. Synthesis, characterization and DNA-binding studies of 1-cyclohexyl-3-tosylurea and its Ni(II), and Cd(II) complexes. *Spectrochim Acta A Mol Biomol Spectrosc* 2008;71:523-528.
- Mohamed GG, Omar MM, Ibrahim AA. Preparation, characterization and biological activity of novel metal-NNNN donor Schiff base complexes. *Spectrochim Acta A Mol Biomol Spectrosc* 2010;75:678-685.
- Patil SA, Naik VH, Kulkarni AD, Badami PS. DNA cleavage, antimicrobial, spectroscopic and fluorescence studies of Co(II),

- Ni(II) and Cu(II) complexes with SNO donor coumarin Schiff bases. *Spectrochim Acta A Mol Biomol Spectrosc* 2010;75:347–354.
12. Senthil Kumar R, Arunachalam S. DNA binding and antimicrobial studies of some polyethyleneimine-copper(II) complex samples containing 1,10-phenanthroline and l-tyrosine as co-ligands. *Polyhedron* 2007;26:3255–3262.
 13. Hussain Reddy K, Sambasiva Reddy P, Ravindra Babu P. Synthesis, spectral studies and nuclease activity of mixed ligand copper(II) complexes of heteroaromatic semicarbazones/thiosemicarbazones and pyridine. *J Inorg Biochem* 1999;77:169–176.
 14. Angelusiu MV, Barbuceanu SE, Draghici C, Almajan GL. New Cu(II), Co(II), Ni(II) complexes with aroyl-hydrazone based ligand. Synthesis, spectroscopic characterization and *in vitro* antibacterial evaluation. *Eur J Med Chem* 2010;45:2055–2062.
 15. Firdaus F, Fatma K, Azam M, Khan SN, Khan AU, Shakir M. Template synthesis and physico-chemical characterization of 14-membered tetraimine macrocyclic complexes, [MLX(2)] [M=Co(II), Ni(II), Cu(II) and Zn(II)]. DNA binding study on [CoLCl(2)] complex. *Spectrochim Acta A Mol Biomol Spectrosc* 2009;72:591–596.
 16. Dean JA, Lange S. *Hand Book of Chemistry*, 14th ed. McGraw-Hill, New York, 1992.
 17. Satyanarayana S, Dabrowiak JC, Chaires JB. Tris(phenanthroline) ruthenium(II) enantiomer interactions with DNA: mode and specificity of binding. *Biochemistry* 1993;32:2573–2584.
 18. Basile LA, Barton JK. Design of a double-stranded DNA cleaving agent with two polyamine metal-binding arms: Ru(DIP)₂Macron⁺. *J Am Chem Soc* 1987;109:7548–7550.
 19. Rabindra Reddy P, Shilpa A. Oxidative and hydrolytic DNA cleavage by Cu(II) complexes of salicylidene tyrosine schiff base and 1,10 phenanthroline/bipyridine. *Polyhedron* 2011;30:565–572.
 20. Li DD, Huang FP, Chen GJ, Gao CY, Tian JL, Gu W et al. Four new copper(II) complexes with 1,3-tpbd ligand: Synthesis, crystal structures, magnetism, oxidative and hydrolytic cleavage of pBR322 DNA. *J Inorg Biochem* 2010;104:431–441.
 21. Zelenko O, Gallagher J, Sigman DS. Scission of DNA with bis(1,10-phenanthroline)copper without intramolecular hydrogen migration *Angew Chem Int Ed Engl* 1997;36:2776–2778.
 22. Tan LF, Chao H, Li H, Liu YJ, Sun B, Wei W et al. Synthesis, characterization, DNA-binding and photocleavage studies of [Ru(bpy)₂(PPIP)]²⁺ and [Ru(phen)₂(PPIP)]²⁺. *J Inorg Biochem* 2005;99:513–520.
 23. Burrows CJ, Muller JG. Oxidative nucleobase modifications leading to strand scission. *Chem Rev* 1998;98:1109–1152.
 24. Raman N, Selvan A. DNA interaction, enhanced DNA photocleavage, electrochemistry, thermal investigation and biopotential properties of new mixed ligand complexes of Cu(II)/VO(IV) based on Schiff bases. *J Mol Struct* 2011;985:173–183.
 25. Psomas G. Mononuclear metal complexes with ciprofloxacin: Synthesis, characterization and DNA-binding properties. *J Inorg Biochem* 2008;102:1798–1811.
 26. Huheey JE, Keiter EA, Keiter RL. *Inorganic Chemistry: Principles of Structure and Reactivity*, Fourth ed. Pearson Education, Inc., New York, 2005.
 27. Azam F, Singh S, Khokhra SL, Prakash O. Synthesis of Schiff bases of naphtha[1,2-d]thiazol-2-amine and metal complexes of 2-(2'-hydroxy)benzylideneaminonaphthothiazole as potential antimicrobial agents. *J Zhejiang Univ Sci B* 2007;8:446–452.